Effects of Pair Correlations in Statistical γ-Decay Spectra

T. Døssing,* T. L. Khoo, T. Lauritsen, I. Ahmad, D. Blumenthal, M. P. Carpenter, B. Crowell, D. Gassmann, R. G. Henry,† R. V. F. Janssens, and D. Nisius

Physics Division, Argonne National Laboratory, Argonne, Illinois 60439

(Received 28 March 1995)

Statistical γ-decay spectra from excited nuclear states are calculated. The spectra reflect the perturbation of the level density by pair correlations and, hence, the stepwise weakening of the pair correlations with increasing quasiparticle number. The level density is obtained by counting many-quasiparticle states from a self-consistent BCS calculation or from a diagonalization of particle number-projected states. The calculated spectra resemble measured spectra from the decay out of superdeformed bands, but have only ~70% of the measured intensity.

PACS numbers: 21.10.Ma, 21.60.Ka, 23.20.Lv, 27.80.+w

Pair correlations are essential for describing many properties of the low-lying states of nuclei. By applying methods developed to describe superfluidity and superconductivity in condensed matter physics, one can explain the observed moments of inertia of ground state rotational bands, as well as the occurrence of a gap in the energy spectrum of even nuclei between the ground and excited states [1]. With increasing temperature, pair correlations become weaker, and are finally completely quenched, in analogy with the superfluid to normal phase transition in liquids. Because of the mesoscopic (i.e., finite) nature of the nucleus, pairing correlations can be appreciably reduced by excitations of only a few quasiparticles, and the superconducting-to-normal phase transition is smeared by fluctuations of the pair correlations.

The subject of the present Letter is the level density ρ of a paired nucleus, treated with explicit counting of quasiparticle excitations. We shall show that the decrease of the pair correlation energy occurs in discrete steps as the number of quasiparticles increases, producing characteristic structures in the nuclear level density as a function of increasing excitation energy U. Statistical decay from a highly excited state will probe the structure of the level density in the states below. Hence, we suggest that an experimental manifestation of such irregularities in the level density may be the occurrence of structures in the spectrum of statistical γ rays. Although the quenching of pairing with increasing temperature is a fundamental property of superconductors, there has been no definitive experimental method to study this phenomenon in nuclear physics. This Letter represents an initial attempt to address this subject, by confronting experimental and theoretical statistical decay spectra emitted from a sharp initial state (instead of from the usual broad initial energy distribution).

Our study is inspired by the recent extraction of the spectrum of γ rays connecting the superdeformed (SD) band and the low-lying states of normal deformation in the nucleus ^{192}Hg [2]. The observed spectrum implies a thermal excitation energy U of 4.3 MeV [2] at the exit point of the SD band, and its quasicontinuous nature supports the proposal [3,4] that the decay is due to the mixing of the SD state with excited compound states of normal deformation. The deduced [4] admixture is very weak, implying mixing with only one or two compound states. Since the compound states deexcite statistically, the decay out of a superdeformed band will, therefore, also proceed as a statistical γ cascade, initiated at one compound state. We shall show that the experimental spectrum is qualitatively reproduced by the calculated one. We propose that structures in the observed decay spectra are due to the effects of pairing in the relevant energy and angular momentum region [$U \sim 0 - 4$ MeV, $I \sim (7 - 11)\hbar$].

As we shall show, the stepwise decrease of the pairing correlations implies a nonmonotonic increase of $\rho(U)$ with U. In contrast, the standard treatment of pairing by means of a partition function [5,6] imposes a monotonic behavior (except at the superfluid to normal phase transition, which lies above the excitation energies of interest here). Level densities resulting from various counting schemes with approximate treatment of pairing [7–9] may display nonmonotonic behavior. However, they have always been executed with slightly higher excitation energies in mind, and often with realistic single-particle levels, with the focus on properties related to the shell structure and the angular momentum. The present calculation is deliberately simple, and employs a schematic treatment (with equivalent level spacings) to elucidate only the major consequences of pairing, which do not depend sensitively on the exact single-particle energies. For the same reason, angular momentum and parity are not explicitly included in the calculation. Thus, we shall be concerned with only general, but not detailed, features of the spectra.

Three different treatments of the pairing interaction are considered, all based on the BCS wave function: (i) the *quasiparticle approximation,* with a self-consistent pair potential; (ii) variation of the energy after *particle-number projection*; and (iii) *diagonalization* within the space spanned by the number-projected states.

 0031-9007/95/75(7)/1276(4)$06.00

The standard BCS wave function with excited quasiparticles can be written

$$|\tau\rangle = \prod_{\nu''\in\tau_2} [v(\nu'') - u(\nu'')a^\dagger(\bar{\nu}'')] \prod_{\nu''\in\tau_1} a^\dagger(\nu') \prod_{\nu''\in\tau_0} [u(\nu) - v(\nu)a^\dagger(\bar{\nu})a^\dagger(\nu)]|\mathcal{N} = 0\rangle . \quad (1)$$

Here, τ_2, τ_1, and τ_0 denote, respectively, the space of double, single, and zero quasiparticle excitations in time-reversed states within the configuration τ. The number of quasiparticle excitations has to match the particle number with respect to being even or odd. [In Eqs. (1) and (2), we follow the notation of Ref. [1].] The Fermi energy λ_τ and the pairing gap Δ_τ are found self-consistently for each configuration, thereby assuring that each configuration can seek its minimum energy. For example, within the quasiparticle approximation, the equation for self-consistency of the average pair field displays how the pairing is weakened by the excitation of quasiparticles:

$$\Delta_\tau = G\langle\tau| \sum_{\nu>0} a^\dagger(\bar{\nu})a^\dagger(\nu)|\tau\rangle = G\left[\sum_{\nu\in\tau_0} u(\nu)v(\nu) \sum_{\nu''\in\tau_2} u(\nu'')v(\nu'')\right]. \quad (2)$$

(Cf. the equivalent equation for the BCS ground state from Ref. [1].) The particle-number projection calculation is carried out in practice by summing over a finite set of gauge angles, as described in Ref. [10]. Diagonalization remedies the nonorthogonality of the different states $|\tau\rangle$. The various approximations can be compared to exact solutions for two cases, that is for equidistant spectra [11] and for the two-level model [12]. For some configurations, the BCS state is too restrictive, and the excitation energies obtained with the quasiparticle approximation or with particle-number projection may be off by about 30%. Diagonalization yields excitation energies of the lowest excited states which are within 4% of the exact value in all cases.

In the following calculations, the standard parameters are chosen to represent a nucleus around ^{192}Hg: equidistant single-particle spectra with respective neutron and proton level spacings $d_n = 0.29$ MeV, $d_p = 0.41$ MeV ($d_n/d_p \approx Z/N$); pairing interactions with strength $G_n = 0.102$ MeV, $G_p = 0.142$ MeV, acting within energy intervals of width $S/2 = 8$ MeV on both sides of the Fermi surface. These values are selected to yield a level density parameter of $a = (\pi^2/3)(d_n^{-1} + d_p^{-1}) = A/10$, where A is the mass number, and proton and neutron pairing gaps in the ground state of even nuclei of magnitude $\Delta_0 = S\exp(-d/G) = 0.9$ MeV.

Figure 1 shows the level densities for even-even N and Z up to 5 MeV. Panel (a) illustrates the unpaired level density, and shows how the contributions from different particle numbers add up to generate a smooth total level density (dashed line), which is well approximated [13] by the standard formula

$$\rho(U) = \frac{\sqrt{\pi}}{12a^{1/4}} U^{-5/4} e^{2\sqrt{aU}} \quad (3)$$

(Eq. 2B-42 of Ref. [14]). With pairing included—see panels (b)–(c) for level densities calculated with the BCS and diagonalization schemes—the smooth behavior is disrupted, principally by a displacement of the level density for a fixed particle number along the energy axis. The pairing energies are displayed in panel (d) of Fig. 1. Because of the jumps in pairing energy from $\mathbf{v} = 0$ to 2 to 4 to 6, etc., the temperature T, defined as $1/T = d\ln(\rho)/dU$, decreases slightly above the energies where the contributions of the $\mathbf{v} + 2$ levels start to add to those of the $\mathbf{v}$ quasiparticle levels. This happens around 1.4 and 3 MeV, as one can check by careful inspection of Fig. 1(c) (and then higher up, around 5.5 MeV). The diagonalization mixes the states with different $\mathbf{v}$ and spreads out their energies, thereby smoothing out the structures, but still leaving kinks in the level density curve, with a decrease in temperature around 1.4 and 3 MeV [Fig. 1(b)].

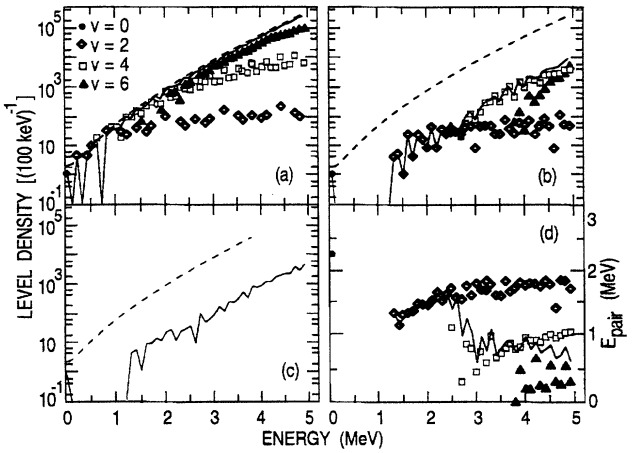

FIG. 1. Level densities (a)–(c) and pair correlation energies (d) for the even-even case. (a) Without pairing; (b) quasiparticle BCS; (c) diagonalization after particle-number projection; (d) BCS. Solid lines in panels (a)–(c) display the total level density, and the average pairing energy in panel (d). The symbols in panel (a) indicate the contributions from different quasiparticle numbers to the level density and to the pairing energy, respectively. Both level densities and pairing energies are binned to 100 keV. For the unpaired and particle-number-projected level densities, all configurations are included. The diagonalization includes all configurations with unpaired excitation energy below 6 MeV, and number-projected energy below 7 MeV. The dashed line is ρ from Eq. (3).

For calculating statistical spectra, the strength function is chosen in accordance with the Axel-Brink hypothesis [15]. For small γ-ray energies on the low energy tail of the giant dipole strength function, a Lorentzian tail just adds another power to the E_γ^3 phase space factor for dipole radiation. With only statistical decay from an excited state at energy U_i, the relative probability for decay to levels at energy U_f is just given by $(U_i - U_f)^4 \rho(U_f)$. Starting from a sharp initial state, the statistical spectrum for decays is computed using level densities calculated with the three schemes discussed above, with a full summation over all initial and final states.

Figure 2 shows statistical decay spectra calculated without [panel (a)] and with pairing [panels (b)–(d)]; in the latter case, the level densities are obtained with diagonalized states for even-even, odd-even, and odd-odd combinations of particle numbers. The initial energy is chosen as $U = 4.3$ MeV, the value deduced [2] for the superdeformed band in ^{192}Hg when it decays out to the normal states. With no pairing, the monotonically increasing temperature of the unpaired level density leads to a smooth statistical decay spectrum; the spectra from the different decay steps are gently displaced relative to each other, combining to form a smooth spectrum for the whole cascade. With pairing, the spectra display strong local fluctuations, which result not only from fluctuations of the level density at low U but also from the high degeneracy of some of the excitations and the underlying equidistant single-particle spectrum. Since the degeneracies are an artifact of the schematic model, we also show spectra smoothed by a Gaussian of width 0.3 MeV.

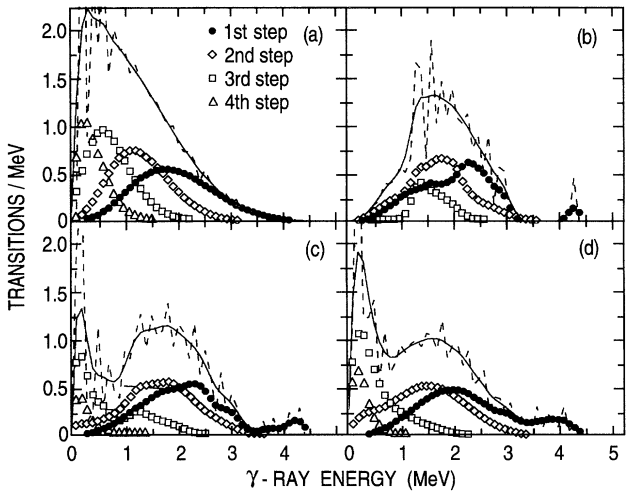

FIG. 2. Statistical decay spectra, with 100 keV bins, for initial energy $U = 4.3$ MeV (dashed lines) calculated with (a) the unpaired even-even level density, and (b)–(d) with the level densities obtained in the diagonalization procedure with (b) even-even, (c) odd-even, and (d) odd-odd particle numbers. The solid lines in the panels are obtained by folding the spectra by a Gaussian function of FWHM = 3 MeV, chosen to be equal to the distance between doubly degenerate neutron single-particle levels. The contributions to the full spectrum from individual cascade steps, denoted by the symbols in panel (a), are also folded by the Gaussian function.

For the even-even nucleus, comparison of the spectra with and without pairing shows that in the former case there is depleted yield for $E_\gamma < 1.2$ MeV, and also between 3.2 and 4 MeV. Both features are due to the pairing gap below the energy for $\mathbf{v} = 2$ quasiparticle excitations. The ensuing compression of the spectrum, together with the last (mainly third) step transitions across the gap to the lowest-lying state, give rise to a broad bump centered around 1.6 MeV. Scrutiny of the different steps of the cascade shows that the compression arises because there is greater overlap of the spectra emitted at each step then for the case without pairing. Furthermore, the spectrum from the first decay step displays two maxima since decay is favored to the energy regions with rapidly increasing level density, around $U = 1.4$ and 3 MeV, just above the onset of the 2 and 4 quasiparticle excitations. Hence, the actual shape of the spectrum reflects perturbations of the level density due to pairing.

For the odd-even and odd-odd cases, there is no gap in the level spectrum, but similar structures in the level densities persist and produce a similar, but less pronounced, bump in the statistical spectrum. This feature, which is absent in the unpaired case, manifests the effects of pairing. However, the filling of the pair gap gives rise to a major difference from the even-even spectrum: there is now appreciable yield at low energy.

The differences in the calculated spectra for even-even, odd-even, and odd-odd nuclei are significant and suggest a direct experimental test of the proposed model. Preliminary comparisons with the measured spectra for decay out of superdeformed bands in ^{192}Hg [2], ^{194}Hg [16], and ^{191}Hg [16] show encouraging qualitative agreement in the overall features. We also predict that the decay spectra from superdeformed bands in the mass 150 region will exhibit less structure than those from the mass 190 region. In the $A \sim 150$ region, the exit spin for the superdeformed bands is around $25\hbar$, where pairing is expected to be strongly quenched, whereas in the $A \sim 190$ region, the exit spin is around $10\hbar$, where pair correlations still persist.

Figure 3(a) illustrates the general dependence of the calculated spectrum on the initial energy as well as on the strength of the pairing interaction. With increasing excitation energy of the initial state, the bump is predicted to grow in intensity, at the same time becoming less steep at its upper edge. This occurs because of the weakening of the pair correlations with increasing U. [In Fig. 3(a) the level density is based on the BCS quasiparticle approximation, since the initial energy 7.5 MeV lies above the cutoff of the basis used for diagonalization.] Figure 3(b) displays how the bump changes with the strength of the pairing interaction. It is seen that the

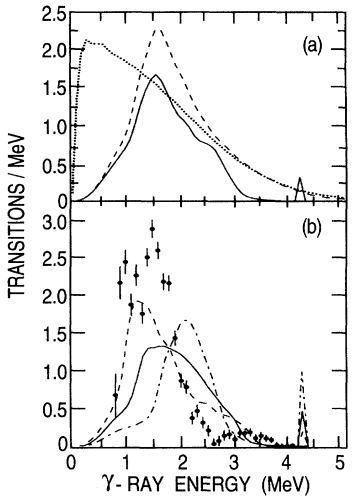

FIG. 3. (a) Statistical decay spectra for initial energy $U = 4.3$ and 7.5 MeV (solid and dashed curves, respectively), calculated with level densities obtained from BCS quasiparticle states for even-even particle number. The dotted curve shows the spectrum with no pairing for $U = 7.5$ MeV. (b) Same as (a), but for level densities from diagonalized states for $U = 4.3$ MeV, with three different strengths of the pairing interaction, parametrized by the ground state pairing gaps $\Delta_0 = 0.7$, 0.9, and 1.1 MeV (dashed, solid, and dot-dashed lines, respectively). All spectra are folded by the same Gaussian function as applied for Fig. 2, except at the upper edge of the spectra. For comparison, the dots with error bars show the experimental decay-out spectrum for ^{192}Hg [2]. The experimental spectrum could not be extracted below 0.8 MeV and terminates at 4.1 MeV, so that the predicted spike at 4.3 MeV could not be confirmed.

maximum of the bump is located at roughly twice the pairing gap Δ_0 of the ground state.

Finally, Fig. 3(b) also shows the experimental decay-out spectrum extracted for ^{192}Hg [2]. Detailed agreement between data and calculation is not expected with the schematic single-particle energies employed. Nevertheless, the clustering of strength around 1.5 MeV is qualitatively reproduced, especially with a pair gap of $\Delta_0 \approx 0.7$ MeV. This value of Δ_0 is below the expected value of 0.9 MeV; this is probably due to the quenching of the pair correlations by angular momentum, which is around $8\hbar$. The calculated spectrum has reduced intensity (multiplicity) compared to the experimental one, but we do not yet have an explanation for this reduction. Since the experimental spectrum stops at 4.1 MeV, we are not able to verify the calculated spike at 4.3 MeV. This spike, which corresponds to a direct transition to the yrast line, has a low multiplicity of 0.05, and is expected to be further reduced by fragmentation from decay to several final states.

γ-ray spectra from thermal neutron capture may also reveal pairing properties in nuclei. Structure has been observed in the γ spectrum following thermal capture to ^{168}Er [17], which is not unlike that seen in the calculated spectrum for $U = 7.5$ MeV [dashed line in Fig. 3(a)]. Early experiments [18,19] also display a bump around 2.5 MeV for rare earth nuclei.

In conclusion, we have demonstrated how the pairing correlation energy in nuclei shows a finite-number effect, decreasing in a steplike manner with increasing excitation energy. This structure is reflected in both the level densities and statistical decay spectra.

Stimulating discussions with R. R. Chasman, P.-H. Heenen, B. Mottelson, and W. Nazarewicz are gratefully acknowledged. This work was supported by the Department of Energy, Nuclear Physics Division, under Contract No. W-31-109-ENG-38.

*Permanent address: The Niels Bohr Institute, University of Copenhagen, Copenhagen, Denmark.
†Present address: Department of Radiology, University of California, San Francisco, CA 94143.

[1] Aa. Bohr and B. R. Mottelson, *Nuclear Structure* (Benjamin, New York, 1975), Vol. II, pp. 641–653.
[2] R. G. Henry *et al.*, Phys. Rev. Lett. **73**, 777 (1994).
[3] E. Vigezzi *et al.*, Phys. Lett. B **249**, 163 (1990).
[4] T. L. Khoo *et al.*, Nucl. Phys. **A557**, 83c (1993).
[5] L. G. Moretto, Nucl. Phys. **A185**, 145 (1972).
[6] M. K. Grossjean and H. Feldmeier, Nucl. Phys. **A444**, 113 (1985).
[7] M. Hillman and J. R. Grover, Phys. Rev. **185**, 1303 (1969).
[8] F. C. Williams, Nucl. Phys. **A133**, 33 (1969).
[9] V. Paar *et al.*, Z. Phys. A **345**, 343 (1993).
[10] P. Ring and P. Schuck, *The Nuclear Many-Body Problem* (Springer-Verlag, New York, 1980).
[11] R. W. Richardson, Phys. Rev. **141**, 949 (1966).
[12] D. C. Zheng, D. W. L. Sprung, and H. Flocard, Phys. Rev. C **46**, 1355 (1992).
[13] T. Ericsson, Adv. Phys. **9**, 425 (1960).
[14] Aa. Bohr and B. R. Mottelson, *Nuclear Structure* (Benjamin, New York, 1969), Vol. I, Appendix 2B.
[15] D. M. Brink, Doctoral thesis, Oxford University, 1955; P. Axel, Phys. Rev. **126**, 671 (1962); Phys. Lett. **4**, 320 (1963).
[16] T. L. Khoo, in Proceedings of the Conference on Physics from Large γ-Ray Detector Arrays, Berkeley, 1994 (to be published); D. Gassman, Diploma thesis, 1995 (unpublished).
[17] D. Visser *et al.*, to be published.
[18] L. V. Groshev *et al.*, *Atlas of Gamma-Ray Spectra from Radiative Capture of Thermal Neutrons* (Pergamon, New York, 1959); Nucl. Data Tables **A3**, 1 (1968); **A5**, 243 (1968).
[19] G. A. Bartholomew *et al.*, Adv. Nucl. Phys. **7**, 229 (1973).